Environmental Monitoring and Assessment (2006) **120:** 109–126
DOI: 10.1007/s10661-005-9052-1 

# HYPERSPECTRAL CHARACTERISTICS OF CANOPY COMPONENTS AND STRUCTURE FOR PHENOLOGICAL ASSESSMENT OF AN INVASIVE WEED

SHAOKUI GE[1,3], JAMES EVERITT[2], RAYMOND CARRUTHERS[3,*], PENG GONG[1] and GERALD ANDERSON[4]

[1]*Center for Assessment and Monitoring of Forest and Environmental Resources, University of California, Berkeley, California, U.S.A.;* [2]*USDA-Agricultural Research Service, Kika de la Garza Subtropical Agricultural Research Center, Integrated Farming and Natural Resources Research Unit, 2413 E Hwy 83, Weslaco, Texas, U.S.A.;* [3]*USDA-Agricultural Research Service, Exotic and Invasive Weeds Research Unit, Western Regional Research Center, Albany, CA, U.S.A.;* [4]*USDA-Agricultural Research Service, Northern Plains Agricultural Research Laboratory, 1500 North Central Avenue, Sidney, Montana, U.S.A.*
*(*author for correspondence, e-mail: ric@pw.usda.gov)*

(Received 7 March 2005; accepted 22 September 2005)

**Abstract.** Spectral reflectance values of four canopy components (stems, buds, opening flowers, and postflowers of yellow starthistle (*Centaurea solstitialis*)) were measured to describe their spectral characteristics. We then physically combined these canopy components to simulate the flowering stage indicated by accumulated flower ratios (AFR) 10%, 40%, 70%, and 90%, respectively. Spectral dissimilarity and spectral angles were calculated to quantitatively identify spectral differences among canopy components and characteristic patterns of these flowering stages. This study demonstrated the ability of hyperspectral data to characterize canopy components, and identify different flowering stages. Stems had a typical spectral profile of green vegetation, which produced a spectral dissimilarity with three reproduction organs (buds, opening flowers, and postflowers). Quantitative differences between simulated flower stages depended on spectral regions and phenological stages examined. Using full-range canopy spectra, the initial flowering stage could be separated from the early peak, peak, and late flowering stages by three spectral regions, i.e. the blue absorption (around 480 nm) and red absorption (around 650 nm) regions and NIR plateau from 730 nm to 950 nm. For airborne CASI data, only the red absorption region and NIR plateau could be used to identify the flowering stages in the field. This study also revealed that the peak flowering stage was more easily recognized than any of the other three stages.

**Keywords:** invasive species, *Centaurea solstitialis*, spectral characteristics, flowering phenological stages, hyperspectral remote sensing

## Introduction

Due to factors linked with increased globalization, especially increases in international trade and exotic species introduction, invasive species have become a serious problem for management of sustainable ecosystems all around the world (Mack and D'Antonio, 1998; Mack *et al.*, 2000; Jackson *et al.*, 2002). Today biological invasions have become the second leading factor causing species endangerment and extinction (Wilcove *et al.*, 1998). It has been estimated that not only are economic

losses huge (estimated at over 200 billion dollars per year), but that damage to natural ecosystems are also extremely large though incalculable (Simberloff, 2001; Mack *et al.*, 2000; Pimentel *et al.*, 2000). Therefore, the massive influx of harmful exotic species is a common central topic of many contemporary conservation biologists and land managers (Simberloff and Stiling, 1996).

Monitoring invaded areas and controlling the corresponding spread of these invaders has attracted a great amount of attention in recent years. Efforts have been made to recognize patches of new invasive species from associated natural or beneficial plants and monitor their distribution and spread as these invasions progress. Assessment of invasive species is a top research priority for natural resource management (Kalkhan and Stohlgren, 2000; Mooney, 1999), including USDA personnel responsible for agriculture and forestry. One of the concerns of those interested in monitoring invasive species is how to use remote sensing to effectively detect infested locations and extract biophysical parameters over a large spatial scale. Although remote sensing techniques have been employed to detect and monitor environmental changes and ecological disasters, traditional multispectral airborne and satellite-borne imagery are often constrained, due to their coarse spectral and spatial resolution (Turner *et al.*, 2003). Recently, hyperspectral remote sensing, which can simultaneous acquire spectral data in many narrow contiguous spectral bands (usually 5–10 nm bands) and thus offers a more detail view of the spectral properties of the intended targets, has been of great interest in natural resource management, and has been used for biodiversity conservation and forest management (Turner *et al.*, 2003; Clark *et al.*, 2004a, b). Hyperspectral remote sensing has shown the potential of recognizing different land surfaces by quantitative comparison of spectral reflectance profiles of land covers such as crops and soils (Price, 1994). Meanwhile, hyperspectral data has been proven a useful information source for detecting invasive species and monitoring their corresponding spread. For example, hyperspectral remote sensing has been successfully used to detect the infestations of leafy spurge (*Euphaorbia esula*) in the Theodore Roosevelt National Park of western North Dakota, USA (Kokaly *et al.*, 2002).

Estimation of plant phenology has been regarded as one of the important aspects of assessing and monitoring natural resources at a large area (Lechowicz, 2001; Chuine and Beaubien, 2001). Traditionally, multispectral images such as the NOAA Advanced Very High Resolution Radiometer (AVHRR) has been used to produce maps of spatial explicit phenological information. Usually, phenological stages determined with multispectral remote sensing include the timing of budbreak, flowering, leafing, fruiting and leaf coloring. However, such phenological information is coarse relative to the invasion estimation and management often needed by local decision makers. For our study, we hypothesize that hyperspectral remote sensing provides a unique and available tool to precisely and remotely estimate such phenological information for a large area, which we hope to demonstrate using the target invasive exotic species, yellow starthistle.

As a winter annual invasive weed, yellow starthistle was first introduced from Eurasia to the United States through California and it now reaches to the east coast, (DiTomaso, 2000). It has already spread to over 20 states and is widely distributed and in very high densities in the western states, especially CA, ID and OR. Such invasions have resulted in a huge economic loss associated with reduction in livestock grazing, altered forage harvesting procedures, lower overall forage yields and a drop in forage quality for range and pasture lands (DiTomaso, 2000). Moreover, this invasive weed reduces wildlife habitat and forage quality, displaces beneficial plants, and decreases the diversity of native plants and animals. In order to control yellow starthistle infestations, a number of control options have been developed and applied for its management, including grazing, mowing, burning, and chemical and biological control. Effectiveness of these methods is closely linked and thus dependent upon the phenological stage of the target weed. This is especially true for the effective use of biological control which involves the release of beneficial insects to damage and control invasive yellow starthistle. It has been shown, that no single method is effective in the control of this weed, thus a long-term sustainable control strategy requires a combination of different control methods (Pitcairn and DiTomaso, 2000). The implementation of such an integrated approach depends upon knowledge, monitoring and/or prediction or the phenological stages in the field (Thomsen *et al.*, 1994, 1996, 1997; DiTomaso, 1997; DiTomaso *et al.*, 1999; Benefield *et al.*, 1999; Pitcairn *et al.*, 1999). For example, studies revealed that biological control is an option to control this weed but demonstrated that the control insects are very sensitive to flower stages (Roché and Roché, 1988; Roché *et al.*, 1997; Roché and Thill, 2001). Since the flowering stage of these weedy plants is a critical factor in mediating plant-insect interaction and biological control, phenological synchrony of introduced insects with the flowering period of yellow starthistle is imperative to successful management (Connett *et al.*, 2001). Additionally, late-season control such as prescribed burning and mowing, and their integration with biological control should be timed such that the plant population has advanced beyond a 2% flower initiation stage (Benefield *et al.*, 1999, 2001). Therefore, estimation of flowering stages is not only important for prediction of population expansion but is also useful for timing other control options (Benefield *et al.*, 2001).

In this study, our objectives are (1) to describe spectral features within 400–2400 nm for different canopy components and simulated flowering stages of yellow starthistle, (2) to quantitatively compare differences among these components as well as simulated flower stages, (3) to determine the potential spectral regions for monitoring flower stages of yellow starthistle, and (4) to compare and test effective spectral regions for monitoring the flower stages with the Compact Airborne Spectrographic Imager (CASI) in the field.

## Methods

### Reflectance measurement for canopy components and simulated flowering stages

When yellow starthistle flowered in late June and early July 2002 along Bear Creek, California (39°00′29″N, 122°22′06″W), four canopy components were randomly collected on July 11, 2002: stems, buds, open flowers, and postflowers. From random patches, we cut and collected 100 stems (about 15 cm from the top of the plants), 100 buds, 100 open flowers, and 100 postflowers. These sample components were separately sealed into plastic bags, immediately put in coolers and then were returned to the laboratory for evaluation after the field sampling was completed (see Figure 1). A full-range field Spec® ProFR Analytical Spectral Devices (ASD) covering 350–2500 nm was used to measure the reflectance for each canopy components and their combinations for four simulated flowering stages, i.e. the initial, early peak, peak, and late flowering stages (Table I). To accomplish this assessment, the 100 stem samples were used as a background to let the simulated canopies sit in the same configuration as when on the living plants with different combinations of buds and flowers (i.e., buds (B), open flowers (F), and postflowers (P)) at different phenological stages, i.e. AFR are 10%, 40%, 70%, and 90%, respectively, in order to assess spectral differences from these combinations buds and flowers. At first, 100 stems were bounded together and kept standing on a black cloth on a table. Then, B, F, and P were combined and uniformly inserted into

*Figure 1.* Canopy components of yellow starthistle: stems (*upper left*), opening flowers (*upper right*), postflowers (*lower left*), and buds (*lower right*).

TABLE I
Canopy combinations for different simulated phenological stages

| Simulated flower stages | Simulated canopy structure | Accumulated flower ratio (AFR) |
|---|---|---|
| Initial flower | B:F:P = 9:1:0 | 10% |
| Early peak flower | B:F:P = 6:3:1 | 40% |
| Peak flower | B:F:P = 3:5:2 | 70% |
| Late flower | B:F:P = 1:3:6 | 90% |

*Note*. (1) B, F, and P stand for buds, open flowers, and postflowers, separately. (2) AFR = (F+P)/(B+F+P), 10, 40, 70, and 90% are the initial, early peak, peak, and late flowering stages, respectively.

the stems bound to simulate canopy flower stages with four different accumulated flowering ratios (AFR), while keeping the same number and condition of stems in the background for every spectral measurement. Here, we assumed that the spectral performance from stems was stable and regarded as background, and the spectral differences primarily resulted from AFR status among weed patches in different flowering stages. Each simulated flowering stage was structured by a total of 100 individual stems and thirty reproduction components with different AFR combinations. In order to have sufficient light for reflectance measurements, two 500W halogen-tungsten filament lamps were set up to simulate natural sunlight and used to illuminate the samples in the laboratory. The reflectance was randomly measured over the sample in the laboratory to keep the spectral sensor at nadir direction with a 25° Field-of-View. The detector was pointed toward the samples and kept 5 cm above them for the duration of the sample. During spectral measurements, every 5–18 min the white reference panel was used to normalize the light condition and thus minimize light differences among the samples. Each sample was organized three times and treated as three replications and 10 readings were taken above the sample for each set. Thus 30 readings were obtained for each treatment combination, as well as simulated canopy combinations. These readings were then averaged and utilized as the spectral characteristics of experimental canopies at simulated phenological stages.

## FIELD CANOPY AND AIRBORNE HYPERSPECTRAL DATA

In order to verify the potential of hyperspectral remote sensing for estimation of spectral patterns of yellow starthistle during these different flowering stages, we followed the Whittaker sampling method designed and developed by Stohlgren *et al.* (1995). We set up two plots in the test field, but improved this method by adding 5 additional subplots of 2 m × 2 m in the middle of these two plots (Figure 2). We investigated canopy AFR in a total of 34 subplots. In our study area, airborne

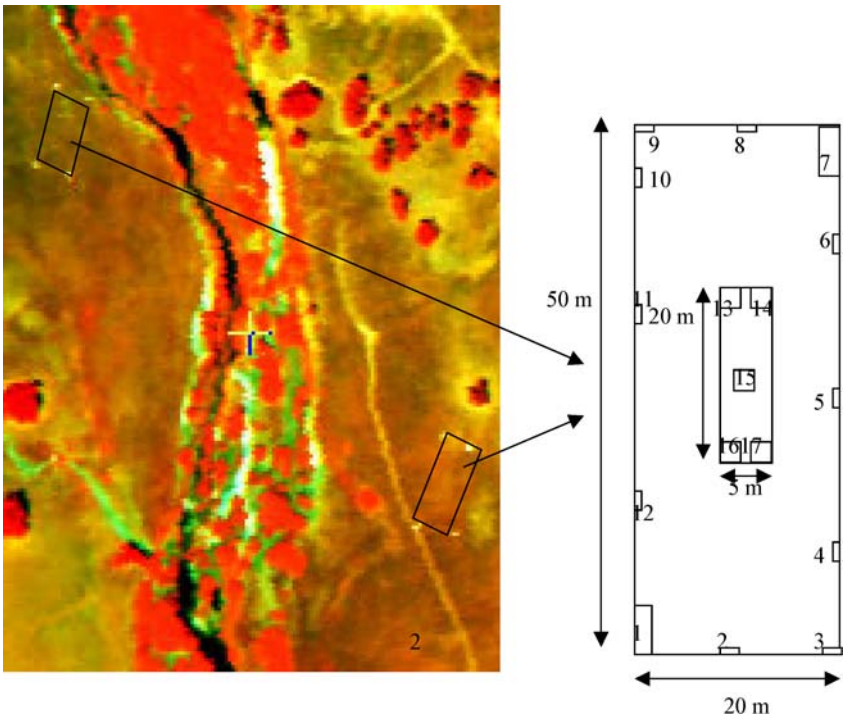


*Figure 2*. Pseudo-color CASI image and field plots. The sizes of subplots 1 and 7 are 2 m × 5 m; 2–6 and 8–12 are 0.5 m × 2 m; 13–17 are 2 m × 2 m.

remotely sensed data (i.e. CASI images) were taken on July 11, 2002 with 2 m spatial resolution by 48 individual narrow bands covering 426.7 nm to 965.1 nm. The bandwidth is between 11.1–11.3 nm. Immediately after the airborne images were taken, the canopy reflectance was measured on the ground by a hyperspectrometer (FieldSpec®ProFR) within each subplot. Canopy reflectance values were then converted into averaged reflectance values within wavelength ranges corresponding to wavebands covered by CASI spectral bands to calibrate CASI data. In parallel with the aerial assessment, AFR were investigated in a 0.5 m × 0.5 m quadrat within each subplot, and included a full accounting of the numbers of buds, open flowers, and postflowers. AFR was then calculated by the accumulated flowered and flowering B divided by the total number of B, F, and P in each quadrat to accurately represent the flowering stage of yellow starthistle plants in the sampled subplots.

## QUANTITATIVE DIFFERENCES AND SPECTRAL POSITIONS AMONG SIMULATED CANOPIES

For each sample, the 30 reflectance readings taken at the laboratory were averaged and regarded as reflectance spectral profiles of each individual canopy component and simulated flowering stage. Here, we used two parameters to quantify the spectral

variability. The first one was to use the root mean square errors (RMS) of their spectra to demonstrate their dissimilarity ($D$) ($S^+$, MathSoft Inc.):

$$D = \left[ \frac{1}{N-1} \sum_{i=1}^{N} [r_1 - r_2]^2 \right]^{1/2}$$

where $r_1$ and $r_2$ are the spectral reflectance in a particular band I, and $N$ is the total number of samples. The second one was spectral angle ($\theta$), which corresponded to the phase difference in the vector space of reflectance spectra.

$$\theta = \cos^{-1} \left[ \frac{\int r_1 * r_2 \, d\lambda}{\left[\int r_1^2 \, d\lambda\right]^{1/2} \left[\int r_2^2 \, d\lambda\right]^{1/2}} \right]$$

These two parameters were calculated at the specific spectral ranges (local) and full range spectrum (overall), respectively. Accordingly, their spectral differences were compared at both these two levels for known degrees to which they were spectrally different and where these differences were located.

### Effective spectral positions with canopy reflectance and CASI imagery

In order to identify effective positions of CASI imagery to estimate different flowering stages, canopy reflectance values measured by SAD were first converted to the averaged reflectance within wavelength ranges to match those bands covered by CASI imagery. These values were used to develop empirical models for calibrating digital numbers of CASI imagery into reflectance-based data. Then, by the correlogram approach, values of both canopy reflectance values and reflectance-based CASI data were used to determine their effective spectral positions where they significantly correlated with AFR. Correlograms were constructed by sequentially regressing reflectance in each band, against AFR. The resulting correlation coefficients (CC) were then plotted against the corresponding wavebands. Finally, potential wavelength ranges were determined by assessing the significance of the CCs.

## Results and Discussion

### Qualitative description

*Spectral Differences Among Canopy Components*

The reflectance spectra of four different canopy components of yellow starthistle showed considerable spectral variation from the visible through the NIR and

mid-infrared to the middle- infrared regions, these variances related primarily to characteristic absorptions, i.e. pigments and water absorptions (Figure 3a). When these spectral regions were magnified or zoomed in, their differences were very apparent.

Within the visible spectrum (400–700 nm), it is generally known that these canopy components are characterized by two types of absorption features, resulting from pigment changes, i.e. chlorophylls and carotenoids. Accordingly, they are called the red and blue absorptions, respectively. Actually, these two types of pigments are often feasible indicators used to assess the phenological stages of plants through hyperspectral remote sensing (Peñuelas and Filella, 1998). In this study, the canopy spectra was found to be within the visible region (Figure 3b), the chlorophyll absorption peaks were located in the red region (630–700 nm), and the carotenoid peaks in the blue region (450–480 nm). The spectrum of stems looks like the typical reflectance spectrum of green plants. Within the visible part of the spectrum, the reflectance was low and dominated by two types of typical absorptions, chlorophylls-causing red absorption was much clear. For the buds, the blue absorption caused by carotenoids was strong compared to that of the stems. On the other hand, the chlorophyll absorption of the buds became weaker than that of stems. This phenomenon showed that relative carotenoid contents in buds increased, while the chlorophyll contents decreased. For the opening flowers, the blue absorption was further increased, over that of the buds. Meanwhile, the chlorophyll absorption continued to decrease and nearly disappeared. For postflowers, the blue absorption still existed, but it weakened in comparison with that found in the flowers, and the chlorophyll absorption was also smaller than this sort of absorption of stems and buds (Figure 3b). These results demonstrated that chlorophyll content decreased when flowers were developing, while the carotenoids increased. Therefore, within the blue and red absorption regions, these four canopy components had different absorption features. Among these four red absorptions, stems had the strongest intensity, while opening flowers had the strongest blue absorption pattern.

Within the near-infrared (NIR) region (Figure 3c), the reflectance was relatively high, and there were three water absorption peaks, centered at 980, 1200, and 1450 nm, respectively. Stems had the highest reflectance over most of the NIR region. For the postflowers, the reflectance on the NIR plateau (730–950 nm) is relatively low, and their water absorptions gradully became weak, probably due to water loss and desiccation after flowering. Within the mid-infrared region (1400–2500 nm), the reflectance of all components was lower than that in NIR, but it was still higher than that in the visible region of the spectra. Within this region, the reflectance was characterized by water content and there were similar reflectance patterns among buds, opening flowers, and postflowers that provided little differentiation.

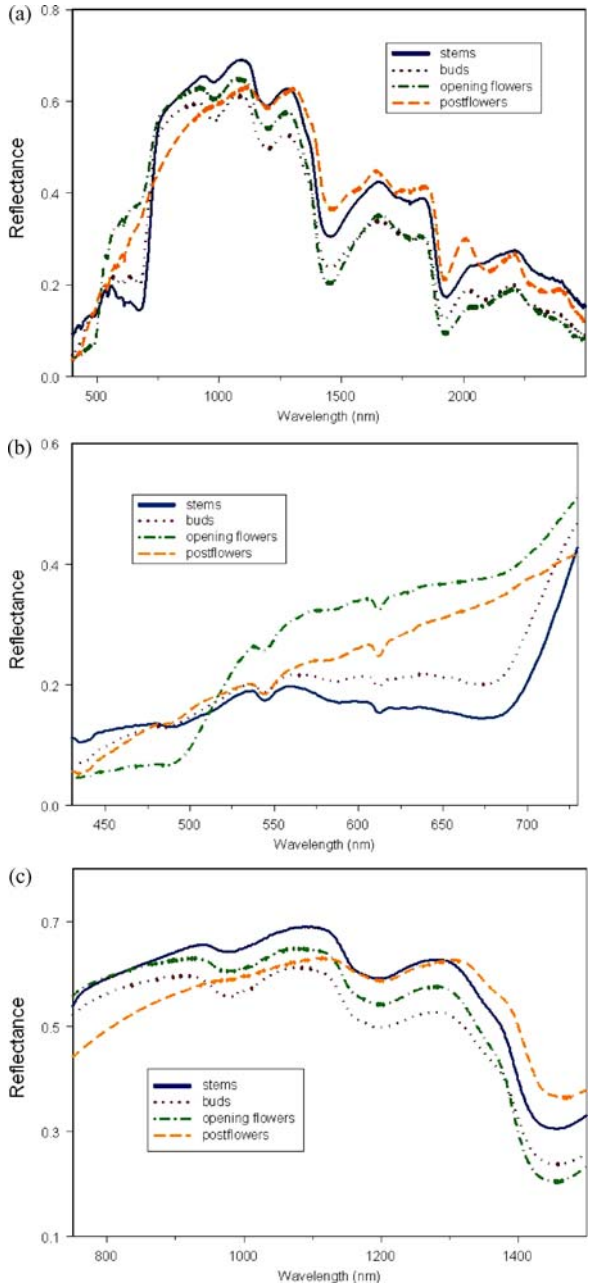


*Figure 3*. Reflectance patterns of different canopy components at (a) the full range from 400–2500 nm, (b) the visible range from 400–750 nm, and (c) the NIR region from 750–1500 nm.

*Spectral Differences Among Simulated Flowering Stages*

The simulated flowering stages at the canopy level, constructed by different proportions of buds, opening flowers, and postflowers, their corresponding ratios of component stages, were characterized as four AFR of 10%, 40%, 70%, and 90%. Among these AFRs, there existed apparent differences among their reflectance spectra (Figure 4a). Within the visible range, the reflectance patterns were dominated by their absorption features among these four simulated flowering stages and thus could be distinguished by this characteristic absorption pattern. Following the increase in percentage of open flowers in the simulated canopies, the blue absorption by carotenoids appeared stronger, and the absorption trough was deepened as canopy aging increased. Therefore, for the simulated canopies, a potential spectral region to discriminate these flowering stages was best located in the blue absorption of the spectrum (Figure 4b). Therefore, it was determined that the earlier stages (AFR = 10% and 40%, respectively) had lower absorption than the later stages (AFR = 70% and 90%, respectively). However, the differences among earlier stages were not clear, e.g. AFR 10% and 40%. Another potential spectral region to aid in identification of these different flowering stages is the red absorption part that is impacted by overall chlorophyll content. Within this region it was difficult to separate 10% AFR from 40% AFR, but the absorption of early could be separated from later stages (70% and 90% AFR).

Within the NIR range from 730 nm to 950 nm, their reflectance values were also different (Figure 4c). In particular, within this part of the spectra, the two earlier flowering stages (10% AFR and 40% AFR) had apparent different spectra; the corresponding absorptions were increased with the increase of flowering stage. Therefore, the NIR spectrum could be used to better quantify development stages and monitor flowering phenology of yellow starthistle. Within the mid-infrared (1700 nm to 2500 nm) region, the simulated combinations of low AFR (including 10% and 40% AFRs) was not easily separated, but they could be distinguished from those stages with higher AFRs (70% and 90%).

## QUANTITATIVE CHARACTERISTICS

*Spectral Characteristics of Canopy Components*

By comparing dissimilarity and spectral angle, different canopy components and simulated flower stages could be quantitatively distinguished (Table II). At the overall level, the stems had the same values of spectral dissimilarity with three kinds of reproduction organs – buds, opening flowers, and postflowers ($D = 0.07$). The spectral dissimilarity of buds to open flowers was smaller than that to postflowers. On the other hand, their corresponding spectral angles were also different. The angle of stems to buds was smaller than to any type of flowers, including opening flowers and postflowers. It was thus concluded that stems and buds had similar spectral phase characteristics, i.e. patterns of absorption and reflectance,

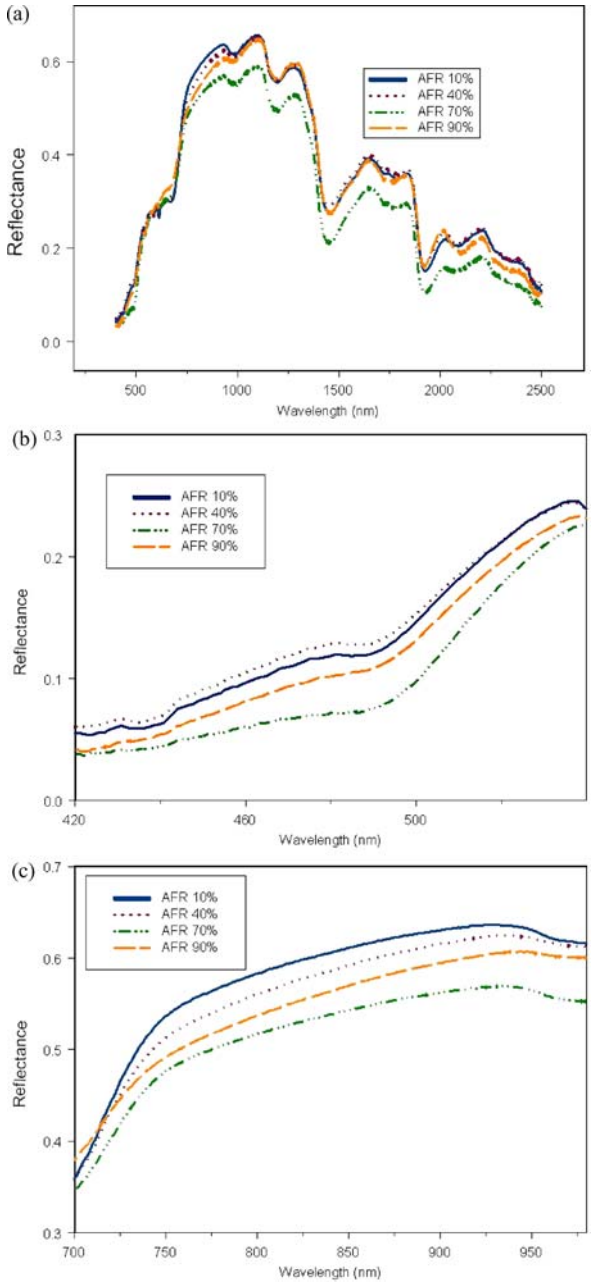


*Figure 4*. Spectral patterns of the simulated canopy at different development stages covering (a) the full range from 400 to 2500 nm, (b) the blue range from 420 to 580 nm, and (c) the NIR plateau from 730 to 980 nm.

TABLE II
The spectral dissimilarity and angles among different canopy components

| | Stems | | Buds | | Opening flowers | |
|---|---|---|---|---|---|---|
| Canopy components | Dissimilarity | Angle | Dissimilarity | Angle | Dissimilarity | Angle |
| Buds | 0.07 | 0.11 | | | | |
| Opening flowers | 0.07 | 0.20 | 0.05 | 0.11 | | |
| Postflowers | 0.07 | 0.14 | 0.08 | 0.17 | 0.09 | 0.22 |

but opening flowers had different spectral patterns from stems, buds, and even postflowers.

Among different canopy components, their dissimilarity changed with the spectral regions (Figure 5a). Although stems had same spectral dissimilarity compared with the other three organs at the overall level (Table II), such dissimilarities were different within individual spectral regions. Spectral dissimilarities of stems with flowers and postflowers mainly existed in the red region. However, there was no apparent dissimilarity between the stems and buds within the visible region, they revealed only minor differences in the NIR and mid-infrared regions from 1000 nm to 2500 nm. In addition, there were also differences in the mid-infrared region between stems and opening flowers. Spectral dissimilarity of buds with flowers significantly appeared in the chlorophyll absorption region, and there was also a small blue absorption between buds and flowers. However, there were no apparent differences in the NIR and mid-infrared regions of the spectra (Figure 5b). This phenomenon revealed that spectral difference between buds and flowers was caused primarily by pigment absorption. The dissimilarity between buds and postflowers located in the red absorption, which meant that their dissimilarity was caused by red absorption. Between buds and postflowers there were three significant peaks of spectral dissimilarity in the NIR and mid-NIR regions, which were due to water absorption (Figure 5b). Although there were small dissimilarities in the visible region between open flowers and postflowers, their difference was much more apparent in the two water absorption regions around 1490 nm and 2000 nm. Clearly, the difference between flowers and postflowers in this spectral region was driven primarily by water content or loss of water as the flowers dried toward mature seedheads (Figure 5c).

*Spectral Characteristics of Simulated Flowering Stages*

Using different combinations of reproductive organs to simulate four canopy flowering stages, i.e. AFR were 10%, 40%, 70%, and 90%, respectively. At the overall level, there existed different dissimilarity among these four simulated stages (Table III). The dissimilarity of the initial flower stage (AFR = 10%) was 0.01, 0.06, and 0.04 with the early peak flower (AFR = 40%), late peak flower (AFR = 70%), and

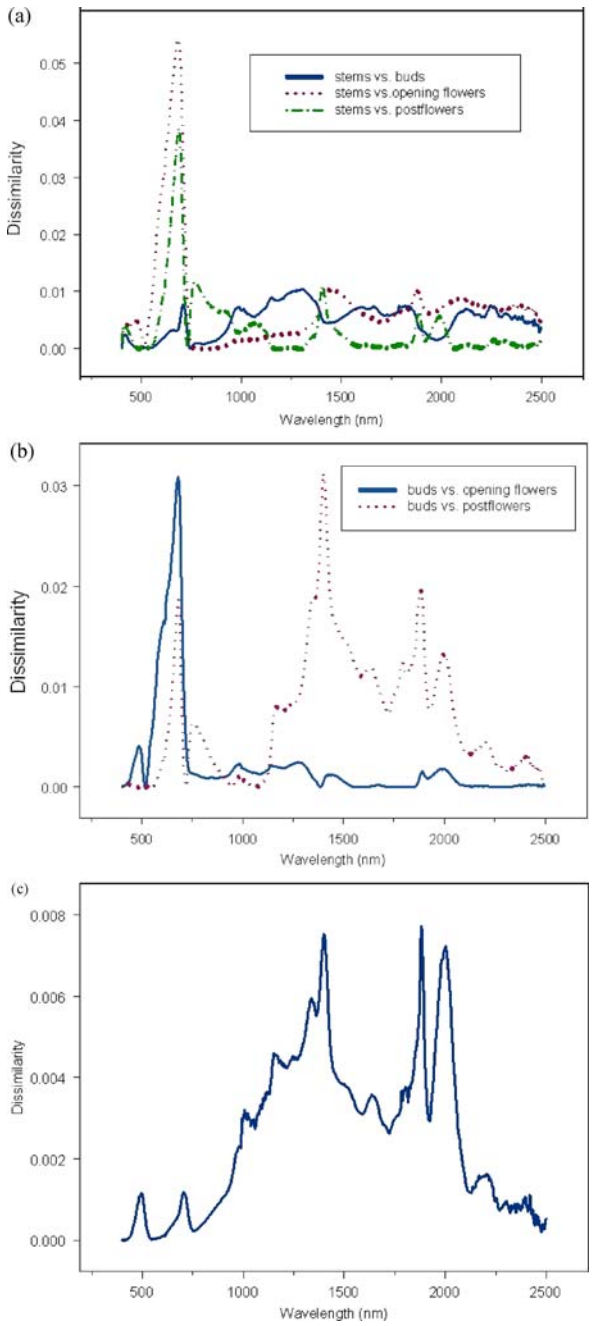


*Figure 5*. The spectral dissimilarity among different organs in various spectral wavelengths: (a) stems with buds, opening flowers, and postflowers, (b) buds with opening flowers and postflowers, and (c) flowers with postflowers.

TABLE III
The spectral dissimilarity and angles among the simulated flowering stages

| | AFR = 10% | | AFR = 40% | | AFR = 70% | |
|---|---|---|---|---|---|---|
| Flower stages | Dissimilarity | Angle | Dissimilarity | Angle | Dissimilarity | Angle |
| AFR = 40% | 0.01 | 0.03 | | | | |
| AFR = 70% | 0.06 | 0.07 | 0.06 | 0.08 | | |
| AFR = 90% | 0.04 | 0.09 | 0.03 | 0.07 | 0.08 | 0.14 |

late flower (AFR = 90%) stages, respectively. The dissimilarity values of the early peak flower were 0.6 and 0.3 with the late peak and late flower periods, respectively. The dissimilarity between the late two periods was 0.08.

For these four simulated flower stages, it was found that values of dissimilarity also depend on spectral regions (Figure 6). For the initial flower stage, there was significant spectral dissimilarity with the other three stages in the blue absorption region and NIR plateau from 730 to 950 nm (Figure 6a). Although the initial flower stage had significant dissimilarity with the late peak flower stage within the mid-infrared region, such dissimilarity disappeared when compared with the other two flower stages, i.e. AFR = 40% and 90%, respectively. Therefore, the initial peak flower stages could be recognized from the other three stages by the blue absorption and reflectance in the NIR plateau. In the meantime, such dissimilarity was much better in the NIR plateau than in the blue region. For the early peak stage (AFR = 40%), it had apparent dissimilarity to the late peak stage (AFR = 70%) in the blue absorption, NIR and mid-infrared regions, but their dissimilarity disappeared in the red absorption areas. There was small dissimilarity between the early peak and late flowering stage, as it was apparent just in the blue and red absorption regions. There was no apparent spectral dissimilarity in the NIR and mid-infrared regions (Figure 6b). In the spectral domain, the late peak flowering stage significantly separated from the stage of AFR 90% by water absorption regions from 1200 to 2100 nm, especially around 1490 nm and 1980 nm. There was no detectable difference between these flowering stages in the visible region (Figure 6c).

## EFFECTIVE SPECTRAL POSITIONS BY CANOPY REFLECTANCE AND CASI DATA

Within the 34 subplots of the two modified-Whittaker field plots, the numbers of buds, flowers and postflowers were investigated for determining their AFR. Canopy reflectance data were also taken to calibrate the digital numbers of CASI images into reflectance-based data. For the full-range canopy reflectance, the correlogram showed that on-site canopy hyperspectral data significantly correlated with AFR

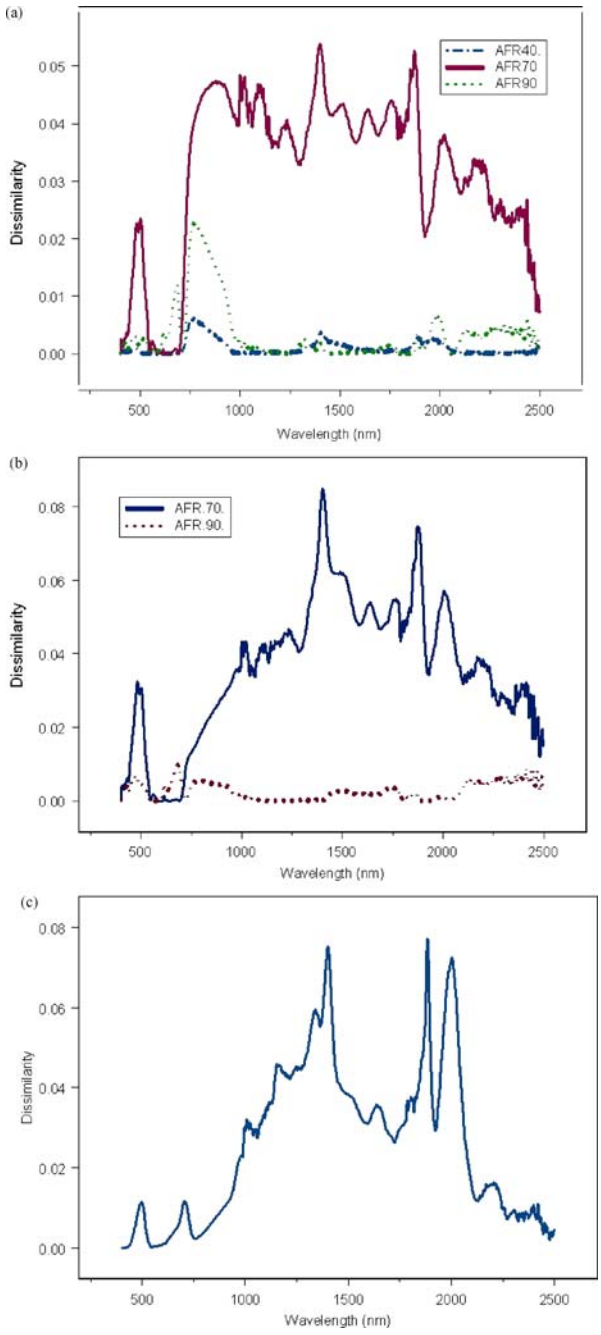


*Figure 6*. The spectral dissimilarity among simulated canopies at different development stages (a) AFR 10% with the other three stages, (b) AFR 40% with AFR 70% and AFR 90%, and (c) AFR 70% with AFR 90%.

within three spectral regions ($n = 34$, $p = 0.001$, $R \geq 0.51$) in the blue absorption, red absorption, and NIR plateau. In particular, within the NIR region such correlation was stronger than those within the blue absorption and red absorption regions. However, after calibrated to reflectance values, airborne remotely sensed data significantly correlated with AFR just within two spectral ranges. They were located in red absorption region centered at 650 nm and in the NIR part, respectively. Compared with on-site canopy reflectance data, the correlation resulting from the blue absorption decreased.

## Conclusion

The results of this study demonstrated the potential of hyperspectral remote sensing for assessing the flowering stages of yellow starthistle under natural field conditions. Four components of the canopy (stems, flower buds, open flowers and postflowers) had unique and characteristic spectral signatures. Stems had a typical reflectance pattern of green vegetation. Significant spectral differences existed among buds, open flowers, and postflowers, and these differences were located in the blue and red absorption regions and NIR region, respectively. With the development from buds through flowers, the blue absorption increased and the red absorption gradually disappeared. The simulated flowering stages (AFR = 10%, 40%, 70% and 90%) showed that two visible absorption regions [e.g. the blue (around 480 nm) and red (around 650 nm) absorption regions] could be used to identify these flowering stages. By canopy reflectance, only within the NIR (730 nm– 950 nm), the initial flower stage (AFR = 10%) might be discriminated from the early peak stage (AFR = 40%). After calibration through on-site canopy reflectance comparison, airborne CASI data showed high correlation with AFR within the red absorption (around 650 nm) and NIR plateau. However, compared with canopy reflectance, the correlation caused by blue absorption decreased. Based on this study, it was concluded that hyperspectral remote sensing data could capture the minor spectral differences among canopy flowering stages using spectral characteristic located in the red absorption region and NIR plateau. Although the blue absorption also showed potential in the *in-situ* canopy reflectance assessment, such trends decreased when using airborne CASI data.

## Acknowledgments

We thank Qi Chen, Desheng Liu, Xin Miao, Le Wang, Jun Yang, and Qian Yu for their help in field sampling. This research was supported by funding from the USDA, ARS (SCA 58-5325-2-0647) and from a research grant from USDA, CSREES (60-5325-1-0360).

## References


Benefield, C. B., DiTomaso, J. M., Kyser, G. B., Orloff, S. B., Churches, K. R., Marcum, D. B. and Nader, G. A.: 1999, 'Success of mowing to control yellow starthistle depends on timing and plant's branching form', *Cal. Agr.* **53**, 17–21.

Benefield, C. B., DiTomaso, J. M., Kyser, G. B. and Tschohl, A.: 2001, 'Reproductive biology of yellow starthistle (*Centaurea solstitialis*): Maximizing late season control', *Weed Sci.* **49**, 83–90.

Chuine, I. and Beaubien, E. G.: 2001, 'Phenology is a major determinant of tree species range', *Ecol. Let.* **4**, 500–510.

Clark, D. B., Carlomagno, S. C., Alvarado, A., Diego, L. and Read, J. M.: 2004a, 'Quantifying mortality of tropical rain forest trees using high-spatial-resolution satellite data', *Ecol. Let.* **7**, 52–59.

Clark, D. B., Read, J. M., Clark, M. L., Cruz, A. M., Dotti, M. F. and Clark, D. A.: 2004b, 'Application of 1-M and 4-M resolution satellite data to ecological studies of tropical rain forests', *Ecol. Appl.* **14**, 61–74.

Connett, J. F., Wilson, L. M., McCafferey, J. P. and Harmon, B. L.: 2001, 'Phenological synchrony of Eustenopus villosus (Coleoptera: Curculionidae) with Centaurea solstitialis in Idaho', *Environ. Entomol.* **30**,439–442.

DiTomaso, J. M.: 1997, 'Risk analysis of various weed control methods', *Proc. Cal. Exotic Plant Pest Coun.* **2**, 61–64.

DiTomaso, J. M., Kyser, G. B. and Hasting, M. S.: 1999, 'Prescribed burning for control of yellow starthistle (*Centaurea solstitialis)* and enhanced native plant diversity', *Weed Sci.* **47**, 233–242.

DiTomaso, J. M.: 2000, 'Invasive weeds in rangelands: Species, impacts and management', *Weed Sci.* **48**, 255–265.

Jackson, R. B., Banner, J. L., Jobbagy, E. G., Pockman, W. T. and Wall, D. H.: 2002, 'Ecosystem carbon loss with woody plant invasion of grasslands', *Nature* **418**, 623–626.

Kalkhan, M. and Stohlgren, T.: 2000, 'Using multi-scale sampling and spatial cross-correlation to investigate patterns of plant species richness', *Environ. Mon. Assess* **64**, 591–605.

Kokaly, R. F., Anderson, G. L. Root, R. R. Brown, K. E., Mladinich, C. S., Hager, S. and Dudek, K. B.: 2002, 'Mapping leafy spurge by identifying signatures of vegetation field spectra in Compact Airborne Spectrographic Imager (CASI) data', *Geol. Soc. Am. Abstr*. **34**, 552.

Lechowicz, M. J.: 2001, 'Phenology. Encyclopedia of Global Environmental Change' Volume 2. *The Earth System: Biological and Ecological Dimensions of Global Environmental Change*, Wiley, London.

Mack, M. and D'Antonio, C.: 1998, 'Impacts of biological invasions on disturbance regimes', *Tren. Ecol. Evol.* **13**, 195–198.

Mack, R. N., Simberloff, D., Lonsdale, W. M., Evans, H., Clout, M. and Bazzaz, F.: 2000, 'Biotic invasions: Causes, epidemiology, global consequences and control', *Ecol. Appl.* **10**, 689–710.

Mooney, H.: 1999, 'The global invasive species program (GISP)', *Biol. Invasions* **1**, 97–98.

Peñuelas, J. and Filella, L.: 1998, 'Visible and near-infrared reflectance techniques for diagnosing plant physiological status', *Trends Plant Sci.* **3**, 151–156.

Pimentel, D., Lach, L., Zuniga, R. and Morrison, D.: 2000, 'Environmental and economic costs associated with non-indigenous species in the United States', *Bioscience* **50**, 53–65.

Pitcairn, M. J. and DiTomaso, J. M.: 2000, 'Rangeland and uncultivated areas: integrating biological control agents and herbicides for starthistle control', in: M. S. Hoddle (ed.), *California Control on Biological Conference II*., pp. 65–72.

Pitcairn, M. J., DiTomaso, J. M. and Fox, J.: 1999, 'Integrating chemical and biological control methods for control of yellow starthistle', in: D. M. Woods (ed.), *Biological Control Program Annual Report*, *1998*. California Department of Food and Agriculture, Plant Health and Pest Prevention Services, Sacramento, CA, pp. 77–82.

Price, J. C.: 1994, 'How unique are spectral signatures?', *Rem. Sens. Envir.* **49**, 181–186.
Silvestri, S., Marani, M., Settle, J., Benvenuto, F. and Marani, A.: 2002, 'Salt marsh vegetation radiometry data analysis and scaling', *Rem. Sens. Envir.* **80**, 473–482.
Roché, C. T. and Roché, B. F.: 1988, 'Distribution and amount of four knapweed (*Centaurea* L.) species in eastern Washington', *Nor. Sci.* **68**, 86–96.
Roché, C. T. and Thill, D. C.: 2001, 'Biology of common crupina and yellow starthistle, two Mediterranean winter annual invaders in western North America', *Weed Sci.* **49**, 439–447.
Roché, C. T., Thill, D. C. and Shafii, B.: 1997, 'Reproductive phenology in yellow starthistle (Centaurea solstitialis)', *Weed Sci.* **45**, 763–770.
Simberloff, D. and Stiling, P.: 1996, 'How risky is biological control?', *Ecology* **77**, 1965–1974.
Simberloff, D.: 2001, 'Biological invasions: How are they affecting us, and what can we do about them?', *West. Nor. Am. Nat.* **61**, 308–315.
Stohlgren, T. J., Falkner, M. B. and Schell, L. D.: 1995, 'A modified-Whittaker nested vegetation sampling method', *Vegetatio* **117**, 113–121.
Thomsen, C. D., Vayssieres, M. P. and Williams, W. A.: 1994, 'Grazing and moving management of yellow starthistle', in: *Proceeding of California Weed Conference* **46**, 228–230.
Thomsen, C. D., Williams, W. A., Olkowski, W. and Pratt, D.W.: 1996, 'Grazing, mowing and clover plantings control yellow starthistle', *The IPM Prac.* **18**, 1–4.
Thomsen, C. D., Vayssieres, M. P. and Williams, W. A.: 1997, 'Mowing and subclover plantings suppress yellow starthistle', *Cal. Agr.* **51**, 15–20.
Turner, W., Spectro, S., Gardiner, N., Fladeland, M., Sterling, E. and Sterninger, M.: 2003, 'Remote sensing for biodiversity science and conservation', *Trends Ecol. Evol.* **18**, 306–314.
Wilcove, D. S., Rothstenm, D., Dubow, J., Phillips, A. and Losos, E.: 1998, 'Quantifying threats to imperiled species in the United States', *Bioscience* **48**, 607–615.